

Unsupervised Representation Learning with Laplacian Pyramid Auto-encoders

Zhao Qilu and Li Zongmin

Abstract—Scale-space representation has been popular in computer vision community due to its theoretical foundation. The motivation for generating a scale-space representation of a given data set originates from the basic observation that real-world objects are composed of different structures at different scales. Hence, it's reasonable to consider learning features with image pyramids generated by smoothing and down-sampling operations. In this paper we propose Laplacian pyramid auto-encoders, a straightforward modification of the deep convolutional auto-encoder architecture, for unsupervised representation learning. The method uses multiple encoding-decoding sub-networks within a Laplacian pyramid framework to reconstruct the original image and the low pass filtered images. The last layer of each encoding sub-network also connects to an encoding layer of the sub-network in the next level, which aims to reverse the process of Laplacian pyramid generation. Experimental results showed that Laplacian pyramid led to a more stable and efficient training procedure and improved the performance of the learned representation with scale information.

Index Terms—Unsupervised representation learning, auto-encoder, scale-space representation, Laplacian pyramid, convolutional neural networks.

1 INTRODUCTION

REAL world objects are meaningful only at a certain scale. You might see an apple perfectly on a table. But if looking at the earth, then it simply does not exist. This multi-scale nature of objects is quite common in nature. Scale-space theory is a framework for early visual operations with complementary motivations from physics and biological vision, which has been developed by the computer vision community to handle the multi-scale nature of image data [1]. It is a formal theory for handling visual structures at different scales, by embedding the original image into a one-parameter family of derived images, in which fine-scale structures are successively suppressed. Scale-space representation has a wide application in computer vision. For example, the scale-invariant feature transform (SIFT) [2], a successful hand-crafted feature in computer vision to detect and describe local features in images, includes an important stage of key localization, which is defined as minima and maxima of the result of difference of Gaussians (DoG) function applied in scale space to a series of resampled and smoothed images.

In consideration of the successful applications of scale-space representation in hand-crafted feature engineering, it's reasonable to apply it in unsupervised representation learning, especially nowadays when supervised deep learning methods have achieved great success in many tasks, owing to its ability to learn features from raw pixels. Recent work (DeCAF) [3] has shown that strong generic feature representations can be extracted from the activation of pre-trained networks. DeCAF defined a new visual feature by concatenating the flattened activations of each layer in the pre-trained networks, which is learned on a set of pre-defined object recognition tasks. This feature has shown strong generalization ability when it's applied to new tasks, which suggests that there exists a generically useful feature representation for natural visual data. However, training deep models in a supervised way needs millions of

semantically-labeled images which cost lots of manual work. Collecting large labeled datasets is very difficult, and there are diminishing returns of making the dataset larger and larger. Hence, unsupervised representation learning has drawn lots of attention for quick access to arbitrary amounts of data, despite its performance is still limited so far.

The most common method used in unsupervised representation learning is an auto-encoder which learns representations based on an encoder-decoder paradigm. An auto-encoder (AE) [4] is an artificial neural network used for unsupervised learning of efficient coding. It consists of two parts, an encoder which outputs a hidden representation and a decoder which attempts to reconstruct the input from the hidden representation. In this paper we propose Laplacian pyramid auto-encoders (LPAE), a straightforward modification of the deep convolutional auto-encoder architecture, for unsupervised representation learning. The motivation for LPAE originates from a basic observation that real-world objects are composed of different structures at different scales. This implies that real-world objects may appear in different ways depending on the scale of observation. Hence, learning feature representations at multiple scales can make learning system robust to the unknown scale variations that may occur. LPAE is different with the traditional auto-encoder that tries to reconstruct its own inputs. LPAE uses multi-path auto-encoders to reconstruct the Gaussian pyramid from the Laplacian pyramid. Each path has connections with next level, which enables a hierarchical encoding strategy mentioned above.

The rest of the paper is organized as follows. In section2, we discuss related works. Section 3 describes the proposed approach. Evaluation of the proposed approach is presented in section 4. Finally, conclusions are presented and future research is discussed.

2 RELATED WORK

Unsupervised representation learning, aiming to use data without any annotation, is a fairly well studied problem in machine learning community. Examples include dictionary learning [5], independent component analysis [6], auto-encoders [4], matrix

• Zhao Qilu and Li Zongmin are with the Department of Computer Applications, China University of Petroleum(East China), Huangdao District, Qingdao, China.
(E-mail:kg19872006@163.com, 734727745@qq.com)

Manuscript received May 1, 2018.

factorization [7], and various forms of clustering [8]. We can use K-means algorithm to group an unlabeled data set into k clusters, whose centroids can be used to produce features [9]. Unsupervised dictionary learning exploits the underlying structure of the unlabeled data to optimize dictionary elements. An example of unsupervised dictionary learning is sparse coding, which aims to learn sets of over-complete bases to represent data efficiently [5].

Recently deep learning methods trained in a supervised way have dramatically improved the state of the art performance on a variety of computer vision tasks. Since supervised deep learning model is capable of learning high-performance visual representations, what about unsupervised deep learning model? Exemplar CNN [10] proposes a method for training Convolutional Neural Networks(convnet) [11] through a surrogate task automatically generated from unlabeled images. DCGAN [12] identified a family of CNN architectures suitable for the adversarial learning framework (GAN) [13] which has a wide application in image generation. The most similar work is LAPGAN [14], which uses Laplacian pyramids with convolutional networks in the context of generative model of images.

Another popular method is to train auto-encoders that learns representations based on an encoder-decoder paradigm. Denoising auto-encoders [15] tries to reconstruct the input from a corrupted version of it, which make the hidden layer discover more robust features. Sparse auto-encoders can learn useful structures in the input data by imposing sparsity on the hidden units during training. Sparsity may be achieved by regularization terms in the loss function [16]. Contractive auto-encoder [17] adds a regularization term in their loss function that makes the model robust to slight variations of input values. By making strong assumptions concerning the distribution of latent variables, variational auto-encoders [18] inherit auto-encoder architecture for learning latent representations. Stacked what-where auto-encoder [19] attempts to learn a factorized representation that encodes invariance and equivariance, and leverage both labeled and unlabeled data to learn this representation in a unified framework. The ladder network [20] contains several lateral shortcut connections from the encoder to decoder at each level of the hierarchy, and the lateral shortcut connections allow the higher levels of the hierarchy to focus on abstract invariant features.

3 APPROACH

The scale-space representation we use is the Laplacian pyramid [21]. After reviewing this, we introduce our LPAE model which integrates multiple deep convolutional auto-encoders into the framework of a Laplacian pyramid.

3.1 Laplacian Pyramid

The Laplacian pyramid is a linear invertible image representation consisting of a set of band-pass images, spaced an octave apart, plus a low-frequency residual. The first step in Laplacian pyramid coding is to low-pass filter the original image g_0 to obtain image g_1 , which is considered a “reduce” version of g_0 since both resolution and sample density are decreased. In a similar way we form g_2 as a reduced version of g_1 , and so on. Filtering is performed by a procedure equivalent to convolution with one of a family of local, symmetric weighting functions. An important member of this family resembles the Gaussian probability distribution, so the sequence of images $[g_0, g_1, \dots, g_n]$ is called the Gaussian pyramid. Suppose we have

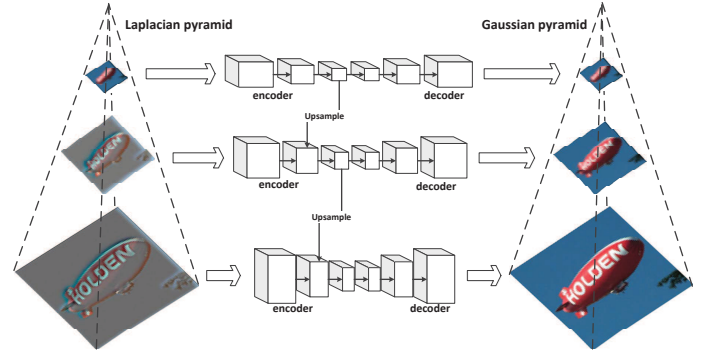


Fig. 1. The architecture of LPAE. LPAE contains multi-path auto-encoders, which are fed with Laplacian pyramids on the left to reconstruct the corresponding Gaussian pyramids on the right.

selected the 5-by-5 generating kernel w , the level-to-level averaging process is performed by the function REDUCE as below:

$$g_l(i, j) = \sum_{m=-2}^2 \sum_{n=-2}^2 w(m, n) * g_{l-1}(2i + m, 2j + n) \quad (1)$$

where i and j denote the coordinate of the pixel.

We define a function EXPAND as the reverse of the function REDUCE. Its effect is to expand an $(M+1) \times (N+1)$ image into a $(2M+1) \times (2N+1)$ image by interpolating new node values between the given values. Thus, the expand function applied to image g_l of the Gaussian pyramid would yield an image g_l' which is the same size as g_{l-1} .

$$g_l'(i, j) = 4 \sum_{m=-2}^2 \sum_{n=-2}^2 w(m, n) * g_l\left(\frac{i-m}{2}, \frac{j-n}{2}\right) \quad (2)$$

Only terms for which $\frac{i-m}{2}$ and $\frac{j-n}{2}$ are integers are included in this sum.

The Laplacian pyramid is a sequence of difference images $[l_0, l_1, \dots, l_n]$. Each is the difference between two levels of the Gaussian pyramid. Thus, for $0 < 1 < n$:

$$l_k = g_k - \text{EXPAND}(g_{k+1}) \quad (3)$$

since there is no image g_{n+1} to serve as the prediction image for g_n , we say $l_n = g_n$.

3.2 Laplacian Pyramid Auto-encoders

Suppose we have a Laplacian pyramid $[l_0, l_1, \dots, l_n]$ and the corresponding Gaussian pyramid $[g_0, g_1, \dots, g_n]$, the aim of our model is to learn a family of hidden representations for the Laplacian pyramid, which can be used to reconstruct the corresponding Gaussian pyramid. A typical architecture of LPAE is shown in Figure 1. We use $E_k()$ and $D_k()$ to denote the encoding network and decoding network at level k , separately. The hidden representation h_k is the output of $E_k()$.

$$h_k = \begin{cases} E_k(l_k, h_{k+1}), & k \neq n \\ E_k(l_k), & k = n \end{cases} \quad (4)$$

For each sub-network, the loss function is as below.

$$\text{loss}_k = \|g_k - D_k(h_k)\|_2 \quad (5)$$

And the total loss is the sum of losses at all levels.

$$\text{loss} = \sum_{k=0}^n \text{loss}_k \quad (6)$$

TABLE 1
The architecture of various models used in the experiments.

4-scales LPAE	convnet				deconvnet			
level 3		3*3*64,1	3*3*64,2	3*3*32,1	3*3*64,1	3*3*64,2	3*3*3,1	
level 2	3*3*128,2	3*3*96,1	3*3*96,1	3*3*64,1	3*3*96,1	3*3*96,1	3*3*128,1	3*3*3,2
level 1	5*5*160,2	5*5*128,1	3*3*96,2	3*3*96,1	3*3*96,1	3*3*128,2	5*5*160,1	5*5*3,2
level 0	5*5*192,2	5*5*160,2	3*3*128,2	3*3*128,1	3*3*128,1	3*3*160,2	5*5*192,2	5*5*3,2
4-scales LAPGAN	convnet				deconvnet			
level 3 <i>D</i>		3*3*64,1	3*3*64,2	3*3*32,1				
level 3 <i>G</i>					3*3*64,1	3*3*64,2	3*3*3,1	
level 2 <i>D</i>	3*3*128,2	3*3*96,1	3*3*96,1	3*3*64,1				
level 2 <i>G</i>	3*3*128,2	3*3*96,1	3*3*96,1	3*3*64,1	3*3*96,1	3*3*96,1	3*3*128,1	3*3*3,2
level 1 <i>D</i>	5*5*160,2	5*5*128,1	3*3*96,2	3*3*96,1				
level 1 <i>G</i>	5*5*160,2	5*5*128,1	3*3*96,2	3*3*96,1	3*3*96,1	3*3*128,2	5*5*160,1	5*5*3,2
level 0 <i>D</i>	5*5*192,2	5*5*160,2	3*3*128,2	3*3*128,1				
level 0 <i>G</i>	5*5*192,2	5*5*160,2	3*3*128,2	3*3*128,1	3*3*128,1	3*3*160,2	5*5*192,2	5*5*3,2
Deep CAE I	convnet				deconvnet			
	5*5*512,2	5*5*512,2	3*3*256,2	3*3*256,1	3*3*256,1	3*3*512,2	3*3*512,2	3*3*3,2
Deep CAE II	convnet				deconvnet			
convnet	5*5*256,1	3*3*128,2	3*3*128,1	3*3*128,1	3*3*128,2	3*3*96,1	3*3*96,2	3*3*96,1
deconvnet	3*3*96,1	3*3*96,2	3*3*128,1	3*3*128,2	3*3*128,1	3*3*128,1	3*3*256,2	5*5*3,1

3.3 Details of the Network Architecture

We use a convnet to encode the input, and employ a deconvolutional net (deconvnet) [22] to produce the reconstruction at each level. All convolutional layers and deconvolutional layers use ReLU nonlinearity. No fully connected layer has been used, which helps handle input data of different size. Each layer is followed by a batch normalization layer. Batch normalization (BN) layer [23] is important for the training of deep models based on the CAE, and we give practical proof in the experimental results. We up-sample the outputs of each convnet, and concatenate them with feature maps of a convolutional layer in the next level. This data flow aims to reverse the process of Laplacian pyramid generation.

4 EXPERIMENTS

To compare our approach to other unsupervised feature learning methods, we report classification results on the STL-10 [9], CIFAR-10 [24] and Caltech-256 [25].

4.1 Datasets

STL-10 contains 96x96 pixel images and relatively less labeled data (5,000 training samples, 100,000 unlabeled samples and 8,000 test samples). It is especially well suited for unsupervised learning as it contains a large set of 100,000 unlabeled samples. In all experiments, we trained our model, Deep CAEs and LAPGAN from the unlabeled subset of STL-10. The CIFAR-10 dataset consists of 60,000 32x32 color images in 10 classes, with 6,000 images per class. There are 50,000 training images and 10,000 test images. Since the resolution of CIFAR-10 images is low, we only evaluated 2-scales LPAE and LAPGAN on CIFAR-10. When testing on Caltech-256, the images were resized to 96*96 pixels, and we randomly selected 30 samples per class for training and used the rest for testing. For all datasets, we repeated the testing procedure 6 times.

4.2 Baselines

In order to evaluate the effectiveness of LPAE, we compared it with the following methods:

- 1) Deep convolutional auto-encoders (DCAE): A standard auto-encoder uses a convnet to encode the input, and employs a deconvnet to produce the reconstruction. We use two types of DCAEs with different architectures in the experiments.
- 2) Laplacian Generative Adversarial Networks (LAPGAN): This method combines the conditional generative adversarial net (CGAN) with a Laplacian pyramid representation to generate natural images in a coarse-to-fine fashion.
- 3) Exemplar CNN: This method has achieved the state of the art result for unsupervised learning on several popular datasets, including STL-10, CIFAR-10, Caltech-101 and Caltech-256. Exemplar CNN used several transformations to obtain surrogate data, and train a convnet to learn features that are invariant to these transformations.
- 4) Other methods for unsupervised representation learning include Convolutional K-means Network (CKN) [26], Hierarchical Matching Pursuit (HMP) [27] and View-Invariant K-means (VIK) [28].

4.3 Experimental Setup

To make a thorough evaluation of our model, we worked with three network architectures of different scales. We have shown the network architecture of 4-scales LPAE on the top of Table 1. By removing the level 3 of 4-scales LPAE, we get 3-scales LPAE. Likewise, we can get 2-scales LPAE. The architectures of deep CAEs are shown at the bottom of Table 1. It's impossible for LPAE and deep CAE to use same architectures. Thus, there is a question for LPAE and deep CAE, whether different performances are coming from the Laplacian pyramid structure, or simply as a result of more or less parameters. In order to

TABLE 2
Classification Performance on Several Datasets (in Percent).

Algorithm	STL10	CIFAR10	Caltech-256(30)	#feature maps
2-scales LPAE	71.9 \pm 0.3	79.4 \pm 0.1	50.3 \pm 0.5	1,088
3-scales LPAE	73.3 \pm 0.1	-	51.7 \pm 0.4	1,472
4-scales LPAE	72.3 \pm 0.3	-	50.9 \pm 0.3	1,632
2-scales LAPGAN	71.0 \pm 0.3	79.2 \pm 0.4	47.2 \pm 0.4	1,088
3-scales LAPGAN	71.4 \pm 0.2	-	48.7 \pm 0.4	1,472
4-scales LAPGAN	70.5 \pm 0.2	-	47.6 \pm 0.5	1,632
Deep CAE I	70.9 \pm 0.4	76.5 \pm 0.1	45.2 \pm 0.3	1,536
Deep CAE II	67.7 \pm 0.1	73.1 \pm 0.2	41.1 \pm 0.2	1,056
Convolutional K-means Network [26]	60.1 \pm 1	82.0	-	8,000
Hierarchical Matching Pursuit [27]	64.5 \pm 1	-	-	1,000
View-Invariant K-means [28]	63.7	81.9	-	6,400
Exemplar CNN [10]	74.2 \pm 0.4	84.3	53.6 \pm 0.2	1,884
Supervised state of the art	87.26 [29]	97.14 [30]	70.6 [31]	-

TABLE 3
Evaluation of features extracted from each level on STL10 (in Percent). “C_level0” means “discard the features extracted from level 0 and use the rest”.

Algorithm	level 0	level 1	level 2	level 3	C_level0	C_level1	C_level2	C_level3	whole set
3-scales LPAE	69.3 \pm 0.1	66.4 \pm 0.3	58.8 \pm 0.1	-	67.4 \pm 0.4	70.2 \pm 0.2	70.6 \pm 0.2	-	73.3 \pm 0.1
4-scales LPAE	69.5 \pm 0.2	64.0 \pm 0.2	60.6 \pm 0.4	43.3 \pm 0.3	65.8 \pm 0.4	68.7 \pm 0.2	68.8 \pm 0.2	71.8 \pm 0.1	72.3 \pm 0.3

disentangle whether the Laplacian pyramid helps or not, we use two deep CAEs with different number of parameters. The number of parameters of deep CAE I is about 16.7M, and the other has about 2M parameters. The 4-scales LPAE shown in Table 1 has almost 4.3M parameters, which is much less than the deep CAE I. This setup would help us make analysis of the question mentioned above. The architecture of LAPGAN is shown in the middle. By removing the top level and the encoding part of the generator of level 2, we can get a 3-scales LAPGAN. For fair comparison, we make LPAE and LAPGAN share same auto-encoders, and the discriminators LAPGAN use encoding part of the corresponding generators. A softmax layer, omitted in Table 1, follows behind the last convolutional layer of each discriminator, the outputs of which are flattened into vectors to feed in the softmax classifier. Each convolutional (deconvolutional) layer is followed by a batch normalization layer. The numbers in each cell denote the size of receptive field, number of feature maps and stride. For example, “3*3*64, 1” means a convolutional (deconvolutional) layer with 3-by-3 receptive field, 64 feature maps and a stride of 1 pixel for each dimension of input. ReLU and BN layers are omitted in the notation.

No pre-processing was applied to training images except ZCA whitening. All models mentioned above were trained with mini-batch Adaptive Moment Estimation (Adam) [32] with a mini-batch size of 50. All weights were initialized from a zero-centered Normal distribution with standard deviation 0.02. Learning rate was set to 0.001 in all models. All models were implemented in TensorFlow 1.3 [33].

At test time we applied the discriminators of LAPGAN, the encoding part of deep CAEs and convnets of LPAE as generic feature extractors. To the feature maps of each convolutional layer we applied the max-pooling method that is commonly used for STL-10 and CIFAR-10 dataset. The pooled features were then flattened into vectors, and we concatenated them to form one unique representation of the image. We trained a

softmax classifier without regularization on these image representations. For all models, max-pooling results in 16 values per feature map.

4.4 Classification Performance and Analysis

We have compared LPAE to several unsupervised feature learning methods, including the current state of the art on each dataset. We also list the state of the art for methods involving supervised feature learning (which is not directly comparable). In Table 2 we report the classification performances of LPAEs, deep CAEs and LAPGANs, that we have achieved in the experiments. The results of the rest are directly cited from the paper [10].

Observations are as follows. First, LPAE and LAPGAN outperformed deep CAEs which didn’t consider the scale-space representation. These improvements didn’t come from the difference of the number of model parameters, because deep CAE I has more parameters. Second, LPAE performed better than LAPGAN. Training LAPGAN is delicate and unstable. As the discriminator got better, the gradient of the generator vanished. The reasons have been theoretically investigated in [34]. In contrary, training LPAEs is stable, especially with the help of BN layers. Third, LPAE methods didn’t achieve the state of the art, but it still outperformed several baselines on STL10 and Caltech-256. Exemplar CNN used various transformations to obtain surrogate data for the CNN training, including scaling the patches by a factor between 0.7 and 1.4. Thus, Exemplar CNN can explore abundant information, which let it learn more discriminative representations. Fourth, both LPAE and LAPGAN performed poor on CIFAR10, which is likely due to the low resolution of CIFAR10 images. Apparently, low resolution fails to provide significant scale-space information. Fifth, the performances of both LPAE and LAPGAN didn’t increase with the number of scales. The down-sampled image at level 3 has a very low resolution, which failed to provide discriminative information as shown in Table 3. It’s clear that

TABLE 4

Evaluation of the influence of representation dimensionality on STL10 (in Percent). “4/” means that we extracted 4 values per feature map to form the representation.

Algorithm	4/	9/	16/	24/
2-LPAE	64.7 ± 0.2	69.2 ± 0.3	71.9 ± 0.3	71.4 ± 0.2
3-LPAE	69.0 ± 0.2	72.1 ± 0.4	73.3 ± 0.1	72.9 ± 0.4
4-LPAE	69.3 ± 0.3	71.5 ± 0.4	72.3 ± 0.3	71.7 ± 0.1
2-LAPGAN	68.4 ± 0.6	70.7 ± 0.4	71.0 ± 0.3	70.5 ± 0.1
3-LAPGAN	69.0 ± 0.6	71.0 ± 0.1	71.4 ± 0.2	70.9 ± 0.4
4-LAPGAN	69.1 ± 0.3	71.1 ± 0.4	70.5 ± 0.2	71.0 ± 0.4
Deep CAE I	68.0 ± 0.4	70.1 ± 0.3	70.9 ± 0.4	70.2 ± 0.1
Deep CAE II	64.6 ± 0.1	66.2 ± 0.3	67.7 ± 0.1	66.9 ± 0.2

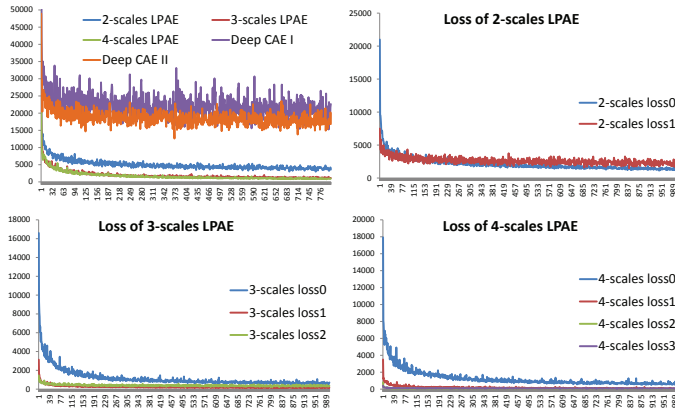


Fig. 2. Loss value against the number of training steps. “2-scales loss0” indicates the reconstruction loss of 2-scales LPAE at level 0.

the classification accuracy dropped slightly when discarding features extracted from level 3, and its performance is also pretty poor. The results shown in Table 3 also indicate that coarser levels perform worse than finer ones, but they still contain their own specific information which is useful for image representation. Besides level of scale, it’s also related with the number of features that the performance of each level dropped as the scale became coarser.

The dimensions of the learned representations had influences on the classification performance as shown in Table 4. Increasing the representation dimensionality would improve the performance at first, but redundant features became more and more, which made the accuracy dropped slightly. As we can see, extracting 9 or 16 values per feature map would be appropriate for the models in the experiments.

4.5 Convergence Analysis

Figure 2 plots the loss value against the number of training steps, and the training procedures of all LPAE models were stopped after 30 epochs. As we can see, the converging speed was very fast for LPAE models, and the training procedure of LPAE was more stable than deep CAE. Besides, the loss of LPAE was much lower than deep CAE, which indicated that LPAE was more suitable for image generation task. The number of scales also had influence on the reconstruction loss. It’s clear that the loss of 2-scales LPAE was larger than the rest of LPAE models. Thus it’s important to choose appropriate number of scales regarding the image resolution. The key idea of this work is to break the learning procedure into successive refinements, which apparently worked well.

TABLE 5

Convergence and BN. The symbol “√” indicates convergence, and the symbol “×” indicates non-convergence.

Algorithm	Adopt BN	Don’t adopt BN
2-scales LPAE	√	×
3-scales LPAE	√	×
4-scales LPAE	√	×
2-scales LAPGAN	√	×
3-scales LAPGAN	√	×
4-scales LAPGAN	√	×
Deep CAE I	√	×
Deep CAE II	√	√

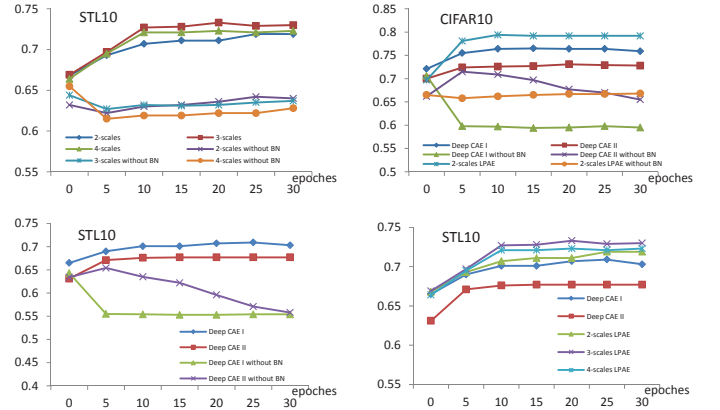


Fig. 3. Top left: LPAE with BN layers VS LPAE without BN layers on STL10; Top right: LPAE VS Deep CAEs on CIFAR10; Bottom left: Deep CAEs with BN layers VS Deep CAEs without BN layers on STL10; Bottom right: LPAEs VS Deep CAEs on STL10.

Adopting BN can help convergence, which is a well known trick in deep learning now. The results in Table 5 confirmed this view, but there was an exception that deep CAE II still converged when removing the BN layers. Figure 3 plots the performance of LPAE and deep CAE (with or without BN layers) against the number of epochs. As we can see, the performances of LPAE and deep CAE achieved the best very fast and stayed stable after 10 epochs. This result is helpful when applying LPAE in practice. BN has a very important influence on the performance of LPAE and deep CAE. The result at epoch 0 in Figure 3 is the performance of random filters. It’s clear that LPAE and deep CAE perform worse than the random filters without BN layers, and using BN layers can lead to a drastic improvement of performance. Again deep CAE II showed a different behavior from other models after removing BN layers. As shown in Figure 3, we can see that its accuracy curve first went up and then went down after removing BN layers, which was different from other models. This phenomenon looks like over-fitting, but it’s hard to believe that over-fitting problem would happen in unsupervised learning. It’s the only difference between deep CAE II with other models that the architecture of deep CAE II is much deeper. Thus one possible explanation is that the deep architecture leads to more powerful learning capability, but also poses the problem of unstable gradients. Thus powerful learning capability made it avoid the training collapse, but unstable gradients led to unstable features. To confirm this view point needs more experiments in depth, and it’s not the major concern of this paper. Thus we leave it to the future work.

5 CONCLUSION

In this paper we embed deep auto-encoders into the framework of Laplacian pyramid, and apply the LPAE model to unsupervised representation learning. Experiments have shown some interesting results which benefit relative research and practical applications of deep auto-encoders approaches. First, scale-space representation like Laplacian pyramid benefitted the image representation learning. Second, for now the auto-encoder framework is more appropriate than generative adversarial nets to combine with Laplacian pyramid for unsupervised representation learning due to more stable training procedure. Third, the number of scales should be set appropriately regarding to the image resolution. Fourth, the learning procedure is efficient that the performances of the learned representations achieved the best very fast. Overall, the key idea of this work is to break the learning procedure into successive refinements, which aims at scale information learning and more stable training.

ACKNOWLEDGMENTS

Thanks for all the supports we have.

REFERENCES

- [1] T. Lindeberg, "Scale-space theory: a basic tool for analyzing structures at different scales," *Journal of Applied Statistics*, vol. 21, no. 1, pp. 225–270, 1994.
- [2] D. G. Lowe, "Object recognition from local scale-invariant features," in *The Proceedings of the Seventh IEEE International Conference on Computer Vision*, ser. ICCV '99. Kerkyra Greece: IEEE, 1999, pp. 1150–1157.
- [3] J. Donahue, Y. Jia, O. Vinyals, J. Hoffman, N. Zhang, E. Tzeng, and T. Darrell, "Decaf: A deep convolutional activation feature for generic visual recognition," in *Proceedings of the 31th International Conference on Machine Learning, ICML 2014, Beijing, China, 21-26 June 2014*, 2014, pp. 647–655.
- [4] H. Bourlard and Y. Kamp, "Auto-association by multilayer perceptrons and singular value decomposition," *Biological Cybernetics*, vol. 59, no. 4, pp. 291–294, Sep 1988.
- [5] H. Lee, A. Battle, R. Raina, and A. Y. Ng, "Efficient sparse coding algorithms," in *Advances in Neural Information Processing Systems 19, Proceedings of the Twentieth Annual Conference on Neural Information Processing Systems, Vancouver, British Columbia, Canada, December 4-7, 2006*, 2006, pp. 801–808.
- [6] A. Hyvärinen and E. Oja, "Independent component analysis: algorithms and applications," *Neural Networks*, vol. 13, no. 4-5, pp. 411–430, 2000.
- [7] N. Srebro, D. M. Rennie, and T. S. Jaakkola, "Maximum-margin matrix factorization," in *Advances in Neural Information Processing Systems 17 [Neural Information Processing Systems, NIPS 2004, December 13-18, 2004, Vancouver, British Columbia, Canada]*, 2004, pp. 1329–1336.
- [8] J. A. Hartigan and M. A. Wong, "Algorithm as 136: A k-means clustering algorithm," *Journal of the Royal Statistical Society*, vol. 28, no. 1, pp. 100–108, 1979.
- [9] A. Coates, A. Y. Ng, and H. Lee, "An analysis of single-layer networks in unsupervised feature learning," in *Proceedings of the Fourteenth International Conference on Artificial Intelligence and Statistics, AISTATS 2011, Fort Lauderdale, USA, April 11-13, 2011*, 2011, pp. 215–223.
- [10] A. Dosovitskiy, P. Fischer, J. T. Springenberg, M. A. Riedmiller, and T. Brox, "Discriminative unsupervised feature learning with exemplar convolutional neural networks," *IEEE Trans. Pattern Anal. Mach. Intell.*, vol. 38, no. 9, pp. 1734–1747, 2016.
- [11] Y. LeCun, B. E. Boser, J. S. Denker, D. Henderson, R. E. Howard, W. E. Hubbard, and L. D. Jackel, "Handwritten digit recognition with a back-propagation network," in *Advances in Neural Information Processing Systems 2, [NIPS Conference, Denver, Colorado, USA, November 27-30, 1989]*, 1989, pp. 396–404.
- [12] A. Radford, L. Metz, and S. Chintala, "Unsupervised representation learning with deep convolutional generative adversarial networks," *CoRR*, vol. abs/1511.06434, 2015.
- [13] I. J. Goodfellow, J. Pouget-Abadie, M. Mirza, B. Xu, D. Warde-Farley, S. Ozair, A. C. Courville, and Y. Bengio, "Generative adversarial networks," *CoRR*, vol. abs/1406.2661, 2014.
- [14] E. L. Denton, S. Chintala, A. Szlam, and R. Fergus, "Deep generative image models using a laplacian pyramid of adversarial networks," in *Advances in Neural Information Processing Systems 28: Annual Conference on Neural Information Processing Systems 2015, December 7-12, 2015, Montreal, Quebec, Canada*, 2015, pp. 1486–1494.
- [15] P. Vincent, H. Larochelle, I. Lajoie, Y. Bengio, and P. Manzagol, "Stacked denoising autoencoders: Learning useful representations in a deep network with a local denoising criterion," *Journal of Machine Learning Research*, vol. 11, pp. 3371–3408, 2010.
- [16] A. Makhzani and B. J. Frey, "k-sparse autoencoders," *CoRR*, vol. abs/1312.5663, 2013.
- [17] S. Rifai, P. Vincent, X. Muller, X. Glorot, and Y. Bengio, "Contractive auto-encoders: Explicit invariance during feature extraction," in *Proceedings of the 28th International Conference on Machine Learning, ICML 2011, Bellevue, Washington, USA, June 28 - July 2, 2011*, 2011, pp. 833–840.
- [18] D. P. Kingma and M. Welling, "Auto-encoding variational bayes," *CoRR*, vol. abs/1312.6114, 2013.
- [19] J. J. Zhao, M. Mathieu, R. Goroshin, and Y. LeCun, "Stacked what-where auto-encoders," *CoRR*, vol. abs/1506.02351, 2015.
- [20] A. Rasmus, M. Berglund, M. Honkala, H. Valpola, and T. Raiko, "Semi-supervised learning with ladder networks," in *Advances in Neural Information Processing Systems 28: Annual Conference on Neural Information Processing Systems 2015, December 7-12, 2015, Montreal, Quebec, Canada*, 2015, pp. 3546–3554.
- [21] P. J. Burt and E. H. Adelson, "The laplacian pyramid as a compact image code," *IEEE Transactions on Communications*, vol. 31, no. 4, pp. 532–540, 1983.
- [22] M. D. Zeiler, D. Krishnan, G. W. Taylor, and R. Fergus, "Deconvolutional networks," in *The Twenty-Third IEEE Conference on Computer Vision and Pattern Recognition, CVPR 2010, San Francisco, CA, USA, 13-18 June 2010*, 2010, pp. 2528–2535.
- [23] S. Ioffe and C. Szegedy, "Batch normalization: Accelerating deep network training by reducing internal covariate shift," in *Proceedings of the 32nd International Conference on Machine Learning, ICML 2015, Lille, France, 6-11 July 2015*, 2015, pp. 448–456.
- [24] A. Krizhevsky and G. Hinton, "Learning multiple layers of features from tiny images," vol. 1, 01 2009.
- [25] G. Griffin, A. Holub, and P. Perona, "Caltech-256 object category dataset," p. 7694, 2007.
- [26] A. Coates and A. Y. Ng, "Selecting receptive fields in deep networks," in *Advances in Neural Information Processing Systems 24: 25th Annual Conference on Neural Information Processing Systems 2011. Proceedings of a meeting held 12-14 December 2011, Granada, Spain.*, 2011, pp. 2528–2536.
- [27] L. Bo, X. Ren, and D. Fox, "Unsupervised feature learning for RGB-D based object recognition," in *Experimental Robotics - The 13th International Symposium on Experimental Robotics, ISER 2012, June 18-21, 2012, Québec City, Canada*, 2012, pp. 387–402.
- [28] K. Y. Hui, "Direct modeling of complex invariances for visual object features," in *Proceedings of the 30th International Conference on Machine Learning, ICML 2013, Atlanta, GA, USA, 16-21 June 2013*, 2013, pp. 352–360.
- [29] T. Devries and G. W. Taylor, "Improved regularization of convolutional neural networks with cutout," *CoRR*, vol. abs/1708.04552, 2017.
- [30] X. Gastaldi, "Shake-shake regularization," *CoRR*, vol. abs/1705.07485, 2017.
- [31] M. D. Zeiler and R. Fergus, "Visualizing and understanding convolutional networks," in *Computer Vision - ECCV 2014 - 13th European Conference, Zurich, Switzerland, September 6-12, 2014, Proceedings, Part I*, 2014, pp. 818–833.
- [32] D. P. Kingma and J. Ba, "Adam: A method for stochastic optimization," *CoRR*, vol. abs/1412.6980, 2014.
- [33] M. Abadi, P. Barham, and et al, "Tensorflow: A system for large-scale machine learning," in *12th USENIX Symposium on Operating Systems Design and Implementation, OSDI 2016, Savannah, GA, USA, November 2-4, 2016.*, 2016, pp. 265–283.
- [34] M. Arjovsky and L. Bottou, "Towards principled methods for training generative adversarial networks," *CoRR*, vol. abs/1701.04862, 2017.